

## Supporting information

### **Continuous-time Binding Kinetics of Graphene Oxide Quantum Dots and Lipid Bilayers Dominated by Hydrogen Bonding: Effect of Nanoparticles' Protein Corona and Membrane Components**

Chaoxiu Ren<sup>a</sup>, Kaili Wang<sup>b</sup>, Xinran Ge<sup>a</sup>, Tao Wu<sup>\*b</sup>, and Qixing Zhou<sup>\*c</sup>

<sup>a</sup>Beijing Key Laboratory of Environmental Toxicology, Department of Toxicology and Sanitary chemistry, School of Public Health, Capital Medical University, Beijing 100069, China.

<sup>b</sup>Beijing Key Laboratory of Enze Biomass Fine Chemicals, College of New Materials and Chemical Engineering, Beijing institute of Petrochemical Technology, Beijing 102617, China.

<sup>c</sup>Key Laboratory of Pollution Processes and Environmental Criteria (Ministry of Education), Tianjin Key Laboratory of Environmental Remediation and Pollution Control, College of Environmental Science and Engineering, Nankai University, Tianjin 300350, China.

\*Corresponding authors:

Tao Wu, Email: [wutao@bipt.edu.cn](mailto:wutao@bipt.edu.cn). Beijing Key Laboratory of Enze Biomass Fine Chemicals, College of New Materials and Chemical Engineering, Beijing Institute of Petrochemical Technology, Beijing 102617, China.

Qixing Zhou, Email: [qxzhou523@163.com](mailto:qxzhou523@163.com). Key Laboratory of Pollution Processes and Environmental Criteria (Ministry of Education), Tianjin Key Laboratory of Environmental Remediation and Pollution Control, College of Environmental Science and Engineering, Nankai University, Tianjin 300350, China.

Total of 17 pages with supplementary materials and methods, 3 tables and 6 figures.

## **Supplementary Materials and Methods**

### **Materials**

L- $\alpha$ -phosphatidylcholine (egg, chicken, PC), cholesterol (ovine wool, Chol), sphingomyelin (egg, chicken, SM), and ganglioside GM1 (ovine brain, GM1) were purchased from Avanti Polar Lipids, Inc. (Alabaster, Alabama, USA). Their two-dimensional (2D) and three-dimensional (3D) structures are shown in Figure S1. HBS-N buffer (150 mM NaCl, 10 mM HEPES, pH 7.4) and L1 sensor chips were purchased from GE Healthcare (Piscataway, New Jersey, USA). Graphene oxide quantum dots (GOQDs) were purchased from XFNANO (product number XF042, Nanjing, Jiangsu, China). Human serum albumin (HSA), potassium bromide (KBr), sodium hydroxide (NaOH) and 3-[(3-cholamidopropyl)dimethylammonio]-1-propanesulfonate (CHAPS) were purchased from Sigma–Aldrich Inc. (Saint Louis, Missouri, USA).

### **Preparation and characterization of small unilamellar vesicles (SUVs)**

To obtain PC1, PC2, PC3, SM4, SM5 and SM6 vesicles, 5 mg of lipids were dissolved in 1 ml of a mixture of organic solvent (methanol: chloroform, 1:2, v/v) at the weight ratios in Table S1. Then, the solvent was removed under a nitrogen stream to initiate the formation of a thin lipid layer on the wall of the glass vial. The film was left in vacuum for 4 hours to remove the remaining organic solvent. The dried lipid film was hydrated and resuspended from the wall of the vial in 1 ml of HBS-N buffer to yield a final concentration of 5 mg/ml large, multilamellar vesicles (LMVs) after vigorous vortexing. The LMV solution was sonicated for 40 min in a bath sonicator (SB-800DTD, SCIENTZ, Ningbo, Zhejiang, China) above the phase transition

temperature ( $T_c$ ) of lipids.  $T_c$  is the critical temperature at which the lipid membrane changes from a gel to a liquid crystal state. To improve the homogeneity of the size distribution, the suspensions were disrupted by 3 freeze–thaw cycles consisting of brief immersion in liquid nitrogen and a 37 °C water bath. The suspensions were forced through a 50 nm polycarbonate filter by an extruder (Avanti Polar Lipids, Inc., Alabaster, Alabama, USA) 11 times to obtain SUVs with a mean diameter of 50-100 nm. The SUV solution was then stored at 4 °C for a maximum of 2 days. The  $\zeta$ -potential and hydrodynamic diameter of SUVs were derived from electrophoretic light scattering (ELS) and dynamic light scattering (DLS) measurements using a Nano Zetasizer (Malvern, Worcestershire, UK). The  $T_c$  of lipids was measured by differential scanning calorimetry (DSC) in the temperature range from -10 °C to 100 °C. The ultraviolet–visible light (UV–Vis) spectrum of SUVs was determined by a UV–Vis spectrophotometer (T90 spectrophotometer, Purkinje General, Beijing, China). The core size of the SUVs was determined by transmission electron microscopy (TEM, Hitachi HT7700, Hitachi, Honshu, Japan).

**Table S1.** Phospholipid composition (weight ratio) used to prepare model membranes.

Lipids	PC1 (%)	PC2 (%)	PC3 (%)	SM4 (%)	SM5 (%)	SM6 (%)
PC	100	83.33	99.01	0	0	0
SM	0	0	0	100	83.33	99.01
Chol	0	16.67	0	0	16.67	0
GM1	0	0	0.99	0	0	0.99

## **Formation of GOQDs-HSA complexes and characterization of GOQDs and GOQDs-HSA**

GOQDs (200 mg/l) and HSA (3.2 g/l) in HBS-N buffer were mixed thoroughly by vortexing. Subsequently, the mixture was shaken for 6 h at 37 °C. Then, the tubes were centrifuged three times (14 800 × g, 10 min) with a 4 °C HBS-N buffer wash between each centrifugation step. Finally, the sedimented GOQDs-HSA were redispersed in HBS-N buffer to obtain the GOQDs-HSA solution. The physicochemical properties of GOQDs and GOQDs-HSA were characterized. The hydrodynamic diameter and  $\zeta$ -potential of QDs were derived from DLS and ELS using a Nano Zetasizer (Malvern, Worcestershire, UK). The absorption spectrum of QDs was determined using a UV–Vis spectrophotometer (T90 spectrophotometer, Purkinje General, Beijing, China). The thickness and core size of the QDs were measured by atomic force microscopy (AFM, Dimension Icon, Bruker, Billerica, Massachusetts, USA) and TEM (Hitachi HT7700, Hitachi, Honshu, Japan), respectively.

## **Preparation and time series AFM measurement of supported lipid bilayer (SLB) interactions with QDs**

By depositing 80  $\mu$ l of SUVs (0.5 mg/ml PC SUVs, 0.1 mg/ml SM SUVs) on a piece of freshly cleaved mica, SLBs were successfully formed. After incubation for 30 min, excess lipids were removed by rinsing the sample with water. The sample was placed in the AFM and imaged to confirm the formation of a bilayer. After obtaining an initial image of the bilayer, 80  $\mu$ l of 100 mg/l GOQDs or GOQDs-HSA was injected into the bilayer. After adding the QDs, continuous time-series images were acquired for 1, 5

and 10 min to observe their effect on the bilayer. Images were analyzed by NanoScope Analysis 1.8 software (Bruker, Billerica, Massachusetts, USA).

### **Surface plasmon resonance (SPR) measurements**

All solutions were filtered through a 0.2  $\mu\text{m}$  filter and degassed by short centrifugation or sonication to minimize the formation of air bubbles. To wash the surface of the L1 chip, 20 mM CHAPS and running buffer were injected in sequence. The interaction of GOQDs or GOQDs-HSA with the membrane was determined at concentrations of 0, 0.1, 0.5, 1, 5, 10, 50 and 100 mg/l, and a distinct SPR cycle was executed for each concentration. Six types of vesicles were tested: PC1, PC2, PC3, SM4, SM5, and SM6. By injecting a 5 mg/ml SUV suspension for 3-15 min in the experimental flow cell, vesicles were immobilized on the surface of the L1 chip. The vesicles completely adsorbed onto the chip surface when the sensorgram flattened out at a constant resonance unit (RU) value ( $>5000$ ). Then, running buffer and 50 mM NaOH were injected successively for 300 s and 60 s. Stabilization was finished by injecting running buffer for 60 s. After stabilization, QD solution was injected for 180 s (association time) followed by running buffer for 300 s (dissociation time). This was followed by the removal of lipids from the chip surface by double injections of CHAPS. Then, the surface of the L1 chip was regenerated by double injections of running buffer for 120 s. The flow rate for the SPR process was 20  $\mu\text{L}/\text{min}$ . A flow cell not covered with SUVs was used as a reference cell. A separate cycle of lipid deposition was used for QDs at each concentration tested. Kinetic analysis of the sensorgrams after subtracting the control value was performed using the two-state curve fitting model (1:1

Langmuir models) by BIAevaluation software version 4.1.1. The binding curve of RU versus QD concentration was fitted to the Hill model using OriginPro 2018. The equation of the Hill model is as follows:

$$y = \frac{1}{1 + 10^{(\log c_{50} - \log c) \cdot h}},$$

where  $y$  represents the binding response,  $c$  represents the concentration of the compound,  $c_{50}$  represents the concentration at which the half-maximal response is reached, and  $h$  represents the Hill coefficient.<sup>1</sup>

### **Fourier transform infrared spectroscopy (FTIR) investigation of lipid interactions with QDs**

After SUVs were allowed to interact with QDs for 10 min, the powders of SUVs, SUVs+GOQDs and SUVs+GOQDs-HSA were freeze-dried using a lyophilizer. Then, the sample tablets were made by mixing the dried samples with KBr (1 mg sample/100 mg KBr). The sample tablets were placed in a Bruker Tensor 27 spectrometer (Bruker, Ettlingen, Germany) purged with dry nitrogen at room temperature, and the FTIR spectra were collected with a resolution of 2 cm<sup>-1</sup> in the range of 400 to 4000 cm<sup>-1</sup>. The recorded FTIR spectra were analyzed using the Bruker software system Opus 6.5 (Bruker, Ettlingen, Germany). 2D-Fourier transform infrared-correlation spectra (2D-FTIR-COS) maps of SLBs interacting with QDs were drawn by Origin 2022 (OriginLab, Massachusetts, USA)

### **MD simulation**

The modeling was performed with packmol software, and the size of the water phospholipid membrane system was  $50 \text{ \AA} \times 50 \text{ \AA} \times 100 \text{ \AA}$ . In the system, PC molecules were uniformly distributed at the center of the box to form a double-layer membrane structure, with a membrane thickness of  $60 \text{ \AA}$ . The rest was filled with a water environment, and the water contains a nanosheet of GOQDs studied. Periodic boundaries were applied in all simulated three-dimensional spaces, and the initial positions of all molecules in the corresponding three-dimensional space were randomly distributed using a Boltzmann distribution. Three different components of phospholipid membranes were investigated, named PC1, PC2, and PC3. Similar modeling methods were used for different phospholipid membranes. Five initial conformations of each phospholipid membrane were constructed, and the one with the lowest energy among the five configurations was selected as the final initial conformation. The initial model of the final water phosphorus lipid membrane system is shown in Figure 5.

To obtain more reasonable dynamic results, the structure is first minimized in energy, followed by a dynamic equilibrium with a step size of 1 fs and a total duration of 50 ns under the canonical ensemble (NVT) ensemble. The temperature was controlled at 298 K using Nose's temperature control method, with a cutoff radius of  $12.5 \text{ \AA}$ . Under the isothermal-isobaric (NPT) ensemble, dynamic simulation was performed at the corresponding temperature, starting from 1 ns and outputting one frame every 200 ps for a total of 500 ns. The pressure control method was Berendsen. The energy curves reached dynamic equilibrium. All dynamics simulations used G53A6 with the Berger lipid force field to explain intermolecular interactions.



In the analysis, the kinetic output included the Z-direction coordinates of the centroid of the nanosheet GOQDs and membrane, and the energy of PC-GOQDs. The intermolecular interaction was calculated using the following formula:

$$E_{interaction}^{nonbonding} = E_{PC-GOQDs}^{nonbonding} - E_{PC}^{nonbonding} - E_{GOQDs}^{nonbonding}$$

## Supplementary Tables

**Table S2.** Hydrodynamic diameter and  $\zeta$ -potential of SUVs by Nano Zetasizer.

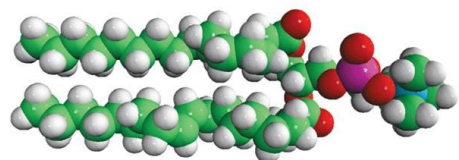
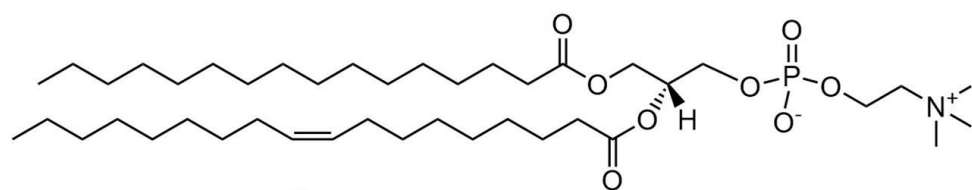
Sample	Hydrodynamic diameter (nm)	$\zeta$ -potential (mV)
PC1	56.80 $\pm$ 0.41	-1.31 $\pm$ 0.11
PC2	83.06 $\pm$ 0.31*	-0.43 $\pm$ 0.03*
PC3	78.02 $\pm$ 0.24*	-0.53 $\pm$ 0.03*
SM4	79.18 $\pm$ 0.17*	-0.34 $\pm$ 0.02*
SM5	104.60 $\pm$ 0.72* * <sub>—</sub>	-2.47 $\pm$ 0.22* * <sub>—</sub>
SM6	74.60 $\pm$ 0.21* * <sub>—</sub>	-6.09 $\pm$ 0.26* * <sub>—</sub>

\* $P < 0.05$ , compared with PC1; \* $P < 0.05$  (SM5 or SM6), compared with SM4.

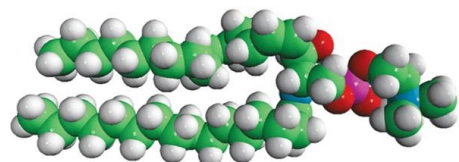
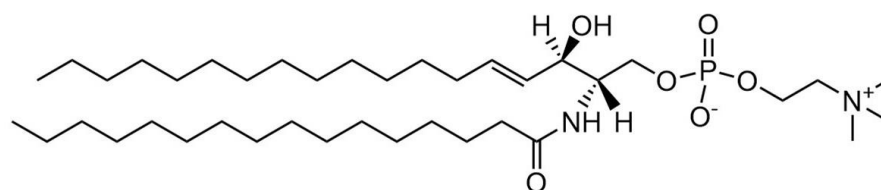
**Table S3.** Lipid affinity expressed as RU50 values of QDs onto PC1, PC2, PC3, SM4, SM5 or SM6 SLBs measured by SPR.

Sample	GOQDs RU50 (mg/l)	GOQDs-HSA RU50 (mg/l)
PC1	0.09	2.71
PC2	3.70	5.31
PC3	3.32	0.09
SM4	0.08	7.71
SM5	0.09	0.09
SM6	0.96	27.68

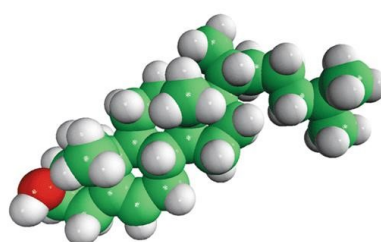
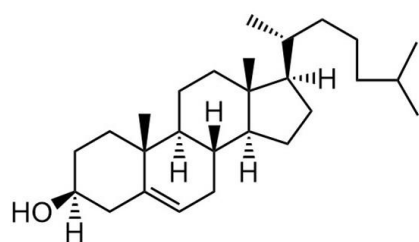
## Supplementary Figures



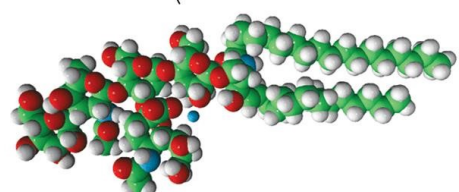
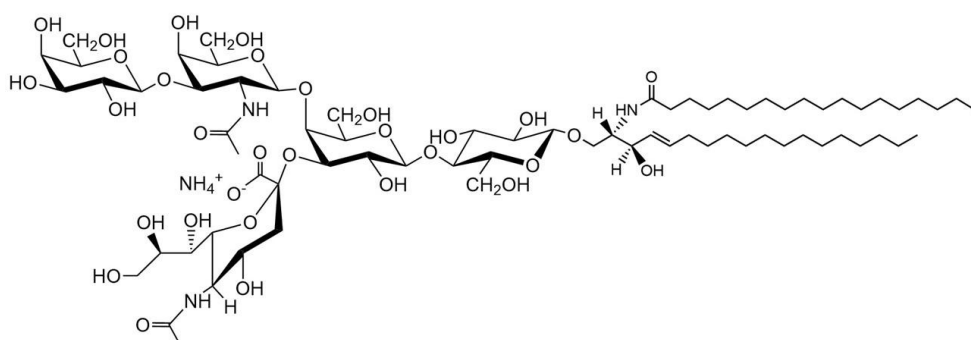
L- $\alpha$ -phosphatidylcholine



Sphingomyelin



Cholesterol



Ganglioside GM1

**Figure S1.** Chemical structures (2D and 3D) of four lipids, PC, SM, Chol and GM1,

used for the formation of supported lipid bilayers in different ratios. PC, L- $\alpha$ -phosphatidylcholine; SM, sphingomyelin; Chol, cholesterol; GM1, ganglioside GM1.

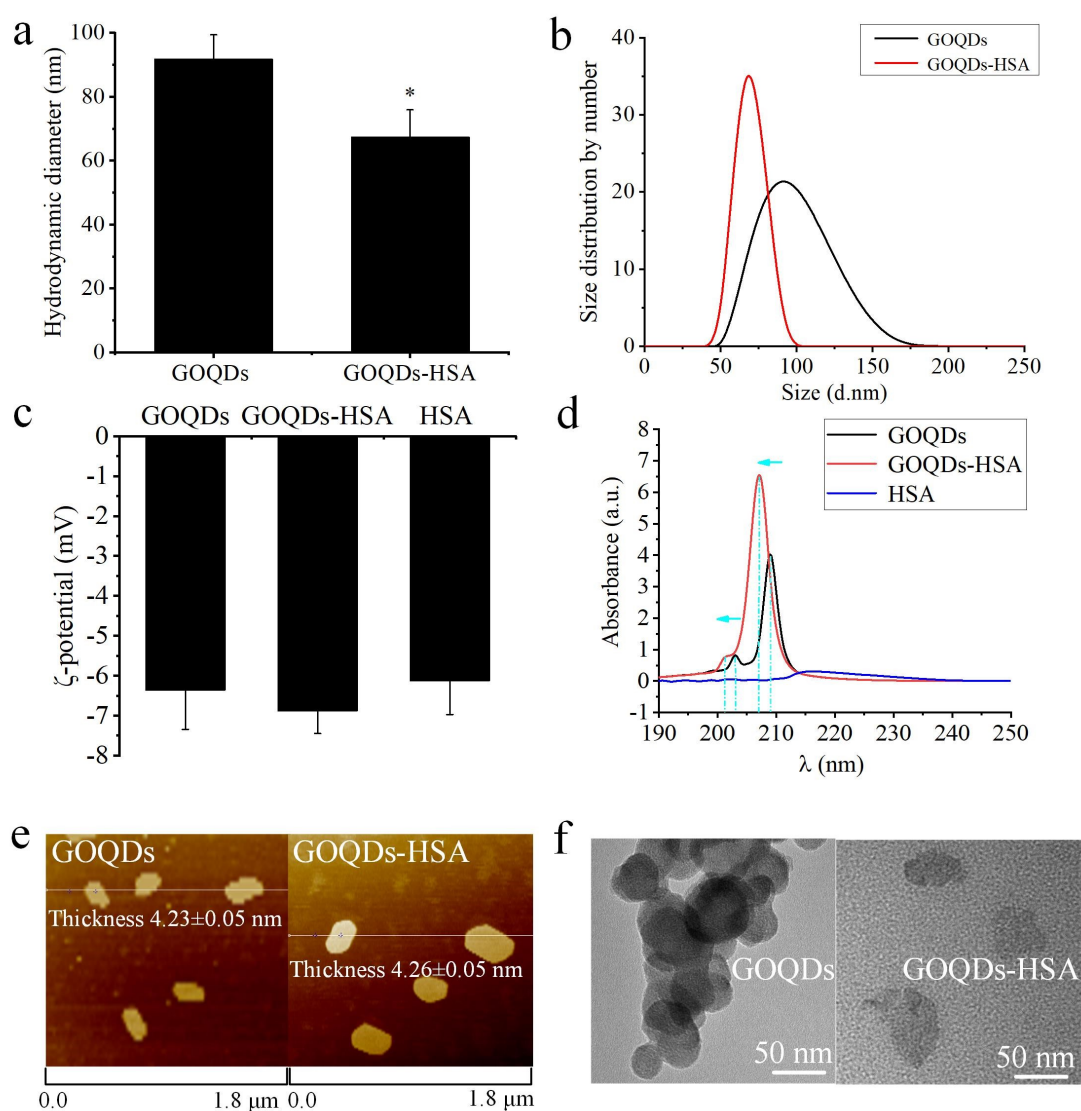


**Figure S2.** Characterization of GOQDs and GOQDs-HSA. (a) Hydrodynamic diameter of GOQDs and GOQDs-HSA. (b) Size distribution of GOQDs and HSA. (c)  $\zeta$ -potential of GOQDs, GOQDs-HSA and HSA. (d) UV-Vis spectra of GOQDs, GOQDs-HSA and HSA. Blue dashed lines and blue arrows denote the absorbance

peak and blueshifts of QDs, respectively. (e) AFM imaging of GOQDs and GOQDs-HSA. (f) TEM imaging of GOQDs and GOQDs-HSA.

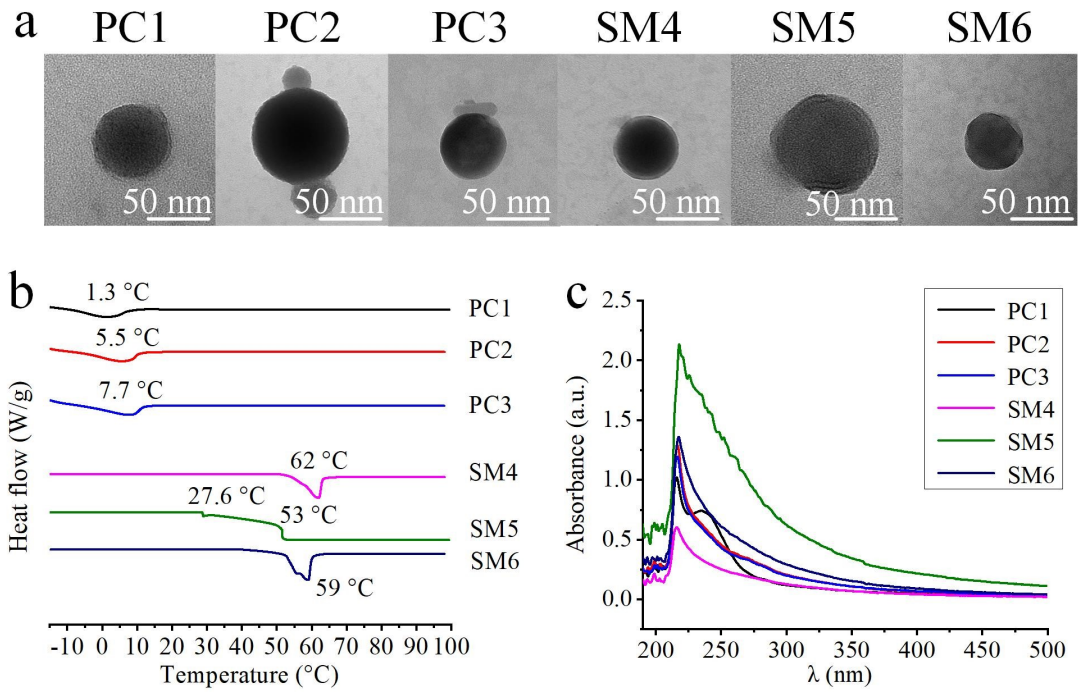


**Figure S3.** Formulation and characterization of SUVs. (a) TEM images of SUVs.

Scale bar: 50 nm. (b) T<sub>c</sub> of lipids by DSC. (c) UV-vis spectra of SUVs.

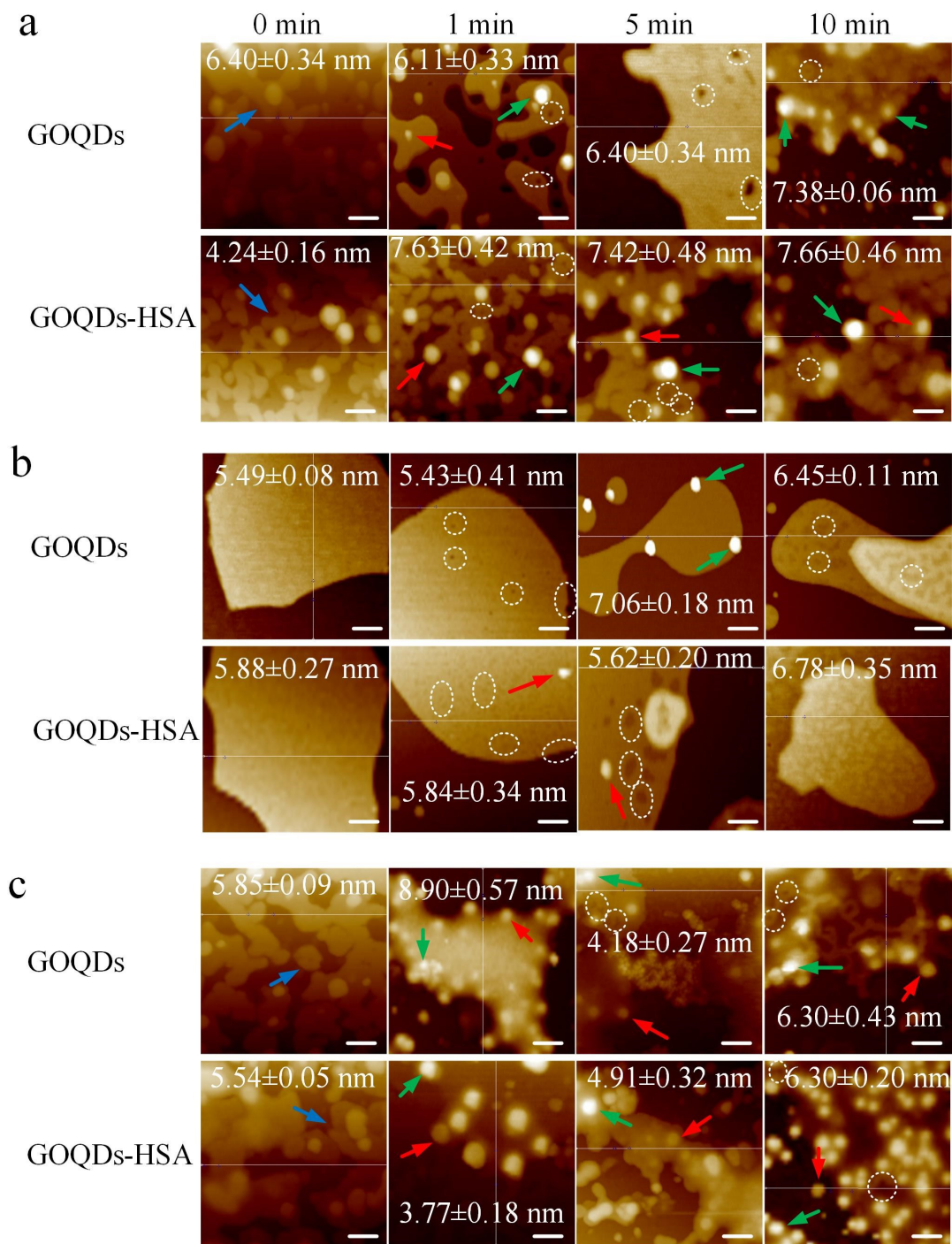


**Figure S4.** Dynamic changes in the SM membrane surface after interacting with QDs imaged by AFM. Dynamic changes in the SM4 (a), SM5 (b) and SM6 (c) membrane surfaces after interacting with QDs. The red arrows indicate QDs on the surface of the membrane, the green arrows indicate the aggregate-like structures, the blue arrows indicate the formed patches, and the white dashed circles indicate holes, pits or other

defects formed in the membrane. Scale bar: 100 nm.

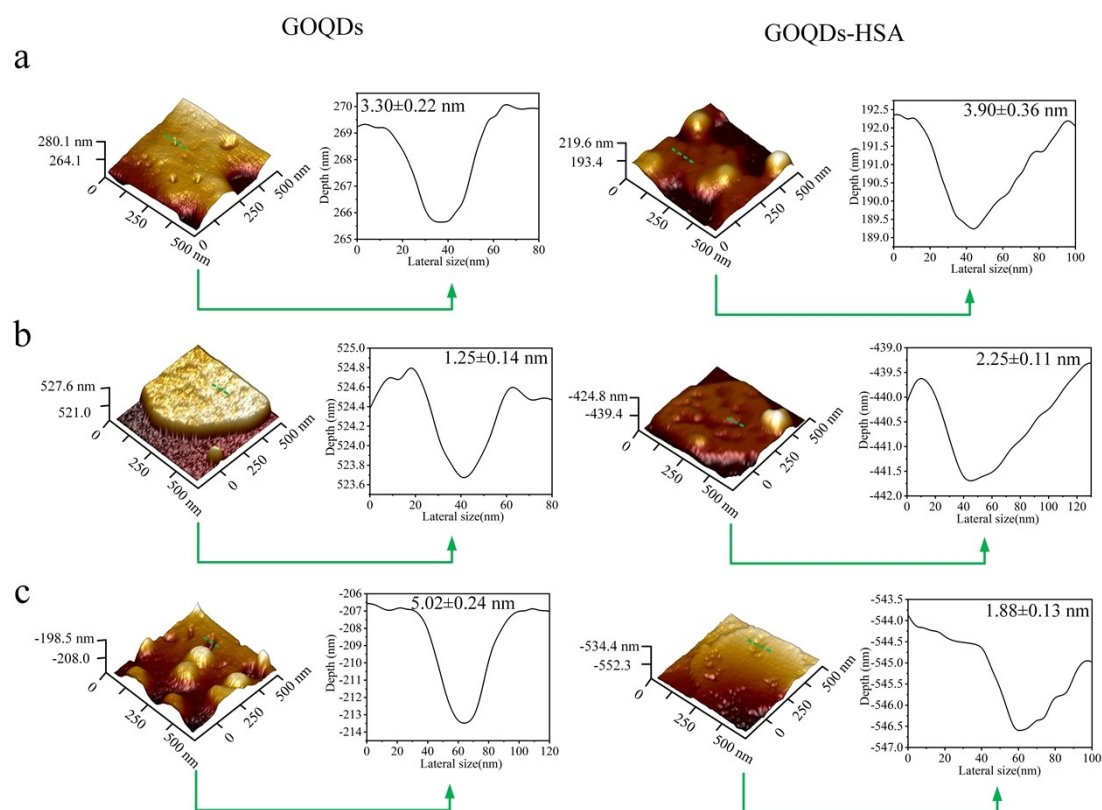


**Figure S5.** Formation and depth of pits on the SM membrane surface after incubation with QDs for 10 min. Formation of pits on the SM4 (a), SM5 (b) and SM6 (c) membrane surfaces and section analysis along the green line.

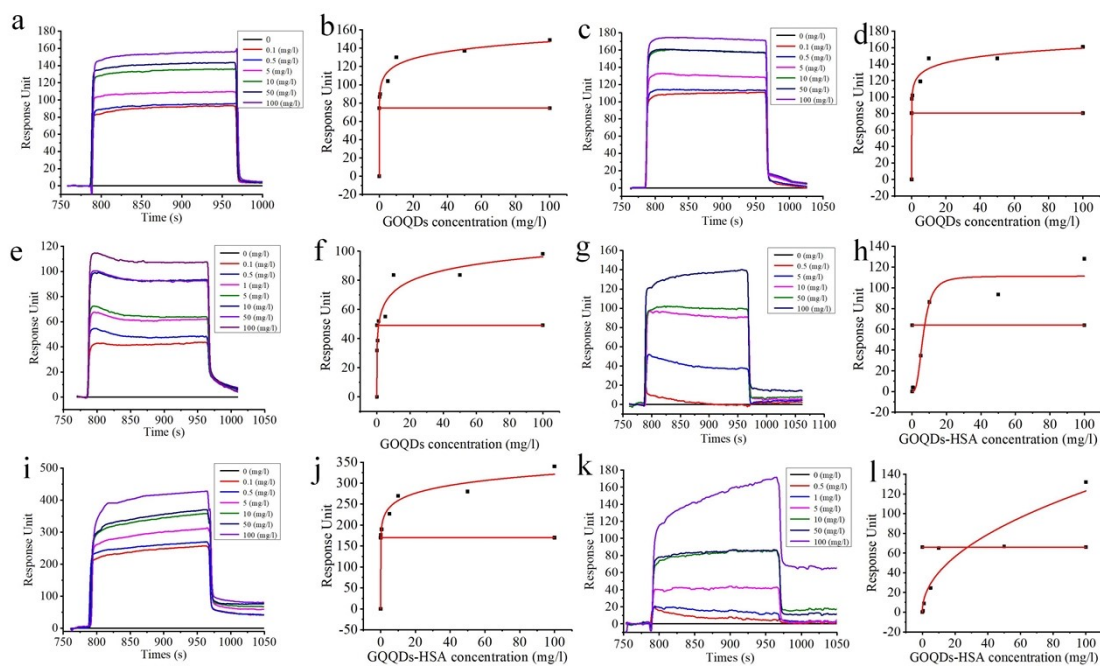


**Figure S6.** Binding curves of RU vs. QD concentration. Concentration-dependent binding of QDs onto SM SLBs measured by SPR and reported as response units (RU) vs. time and RU vs. QD concentration. The operation processes of the interaction between QDs and SM SLBs by SPR were the same as those of PC SLBs, as shown in the legend of Figure 3. Binding curves of GOQDs (0, 0.1, 0.5, 5, 10, 50, 100 mg/l) onto SM4 (a), SM5 (c) and SM6 (e) SLBs. Fitting curves of GOQD binding onto SM4 (b), SM5 (d) and SM6 (f) SLBs by the Hill model. Binding curves of GOQDs-HSA (0, 0.5, 5, 10, 50, 100 mg/l) onto SM4 (g), SM5 (i) and SM6 (k) SLBs. Fitting curves of GOQDs-HSA binding onto SM4 (h), SM5 (j) and SM6 (l) SLBs by the Hill model. The red curves are fitting curves of QDs onto SLBs by the Hill model (b, d, f, h, j and l). The abscissa value of the intersection point of the red curve and the red line is the RU50 value (b, d, f, h, j and l).



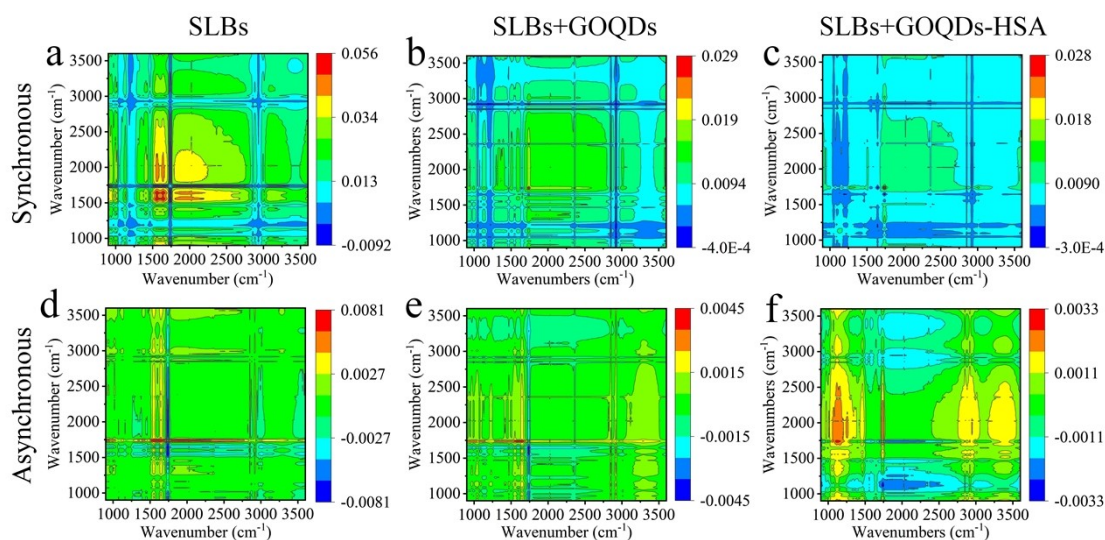


**Figure S7.** 2D-Fourier transform infrared-correlation spectra (2D-FTIR-COS) maps of SLBs interacting with QDs. Synchronous 2D-FTIR-COS maps of SLBs (a), SLBs interacting with GOQDs (b) or GOQDs-HSA (c). Asynchronous 2D-FTIR-COS maps of SLBs (d), SLBs interacting with GOQDs (e) or GOQDs-HSA (f).

## References

- 1 K. Segers, O. Sperandio, M. Sack, R. Fischer, M. A. Miteva, J. Rosing, G. A. F. Nicolaes and B. O. Villoutreix, Design of protein-membrane interaction inhibitors by virtual ligand screening, proof of concept with the c2 domain of factor  $\nu$ , *Proc. Natl. Acad. Sci. U. S. A.*, 2007, **104**, 12697-12702.